Binding Dynamics and Electron Transfer between Plastocyanin and Photosystem I†

Friedel Drepper,‡ Michael Hippler,§ Wolfgang Nitschke,|| and Wolfgang Haehnel*

Lehrstuhl für Biochemie der Pflanzen, Institut für Biologie II, Albert-Ludwigs-Universität, Schänzlestrasse 1, D-79104, Freiburg, Germany

Received June 29, 1995; Revised Manuscript Received November 9, 1995⊗

ABSTRACT: The mechanism of the electron transfer from the soluble protein plastocyanin to the multiprotein complex of photosystem I from spinach has been studied in detail. The two kinetic components of $P700^+$ reduction by plastocyanin after a laser flash, showing a constant half-life of 11 μs and a variable half-life of the second-order reaction, respectively, are used to monitor the electron transfer from bound and soluble plastocyanin. The effect of increasing concentration of reduced plastocyanin on both of these kinetic components and the competition by oxidized plastocyanin is used to estimate the individual dissociation constants of the complex between the proteins in each of its oxidized and reduced state. The dissociation constant of oxidized plastocyanin is about six times larger than that of 7 μM found for reduced plastocyanin and purified PSI. Consistent with this result the midpoint redox potential of plastocyanin bound to photosystem I either in equilibrium with soluble plastocyanin or after cross-linking to photosystem I is found to be 50−60 mV higher than that of soluble plastocyanin. It is concluded that the driving force of the intracomplex electron transfer is decreased in favor of an optimized turnover of photosystem I. Double-flash excitation shows that oxidized plastocyanin has to leave the complex after the electron transfer before a new reduced plastocyanin molecule can bind to photosystem I. This release of oxidized plastocyanin with a half-life of about 60 μs limits the turnover of photosystem I. All data are consistently described by a model including the formation of a complex at a single binding site of photosystem I. Differences in the rate and binding constants are discussed with respect to the structure and the electrostatic and hydrophobic interactions stabilizing the complex as well as their modification by the membrane environment *in situ*.

Photosynthetic as well as respiratory electron transport chains involve two significantly different processes: (i) the intraprotein electron transfer between redox cofactors arranged within the stable structure of electron transfer complexes and (ii) the interprotein electron transfer involving mobile proteins which have to diffuse and bind to the reaction partner. The understanding of the intraprotein electron transfer has been remarkably increased by knowledge of the structure of the purple bacterial reaction centers (Deisenhofer et al., 1985; Allen et al., 1987) and by the basic electron transfer theory (Marcus & Sutin, 1985). Both stimulated detailed studies of electron transfer steps [for a review see Boxer (1990)] and their dependence on driving force and distance (Gunner & Dutton, 1989; Moser et al., 1992; Lin et al., 1994). During the binding process a properly oriented pair of the redox partners has to be formed to optimize the interprotein electron transfer between the active sites, a process which is not fully understood (Marcus & Sutin, 1985; Venturoli et al., 1993). A detailed knowledge of the binding mechanism and of the redox midpoint potential of the reaction partners in the transient complex is prerequisite for an understanding of these electron transfer reactions. The electron transfer between soluble electron carriers and photosynthetic reaction centers as that between plastocyanin (Pc)[1] and photosystem I (PSI) or the analogous one between cytochrome (cyt) c_2 and the reaction center in purple bacteria can be triggered by short pulses of light. These reaction partners present suitable systems for a detailed study of the electron transfer process.

Pc is a 10 kDa type I copper protein. It transfers electrons in the thylakoid lumen from cyt *f* in the cyt *bf* complex to photooxidized P700 in PSI. The structure has been resolved for oxidized and reduced poplar Pc at high resolution (Guss & Freeman, 1983; Guss et al., 1986) and was found to be conserved in several other species (Moore et al., 1988, 1991; Collyer et al., 1990; Redinbo et al., 1993). Two conserved regions have been identified as recognition and binding sites at the surface of the molecule, a flat hydrophobic region including the copper ligand His87 and a negative region of two patches adjacent to Tyr83. While Tyr83 has been concluded to be involved in the electron transfer from cyt *f* (He et al., 1991), it is His87 *via* which the electrons are transfered to $P700^+$ (Sykes, 1990; Nordling et al., 1991; Haehnel et al., 1994). The binding of Pc to PSI does not only involve electrostatic interactions [Bengis & Nelson, 1977; *cf.* Haehnel (1986)] but also the flat hydrophobic surface (Haehnel et al., 1994).

† This work was supported by Deutsche Forschungsgemeinschaft Ha 1084/5-3 and SFB 388 and by the European Community Contract No. BIO2CT-930076.

* Address correspondence to this author.

‡ Present address: Département de Biologie, C. E. de Saclay, Service BPH, F-91190 Gif-sur-Yvette, France.

§ Present address: Département de Biologie Moléculaire, Université de Genève, 30 Quai Ernest Ansermet, CH-1211 Genève, Switzerland.

|| Present address: BIP-CNRS, 31, Chemin Joseph-Aiguier, F-13402 Marseille Cédex 20, France.

⊗ Abstract published in *Advance ACS Abstracts,* December 15, 1995.

[1] Abbreviations: Chl, chlorophyll; Cyt, cytochrome; DAD, diaminodurene; FWHM, full width at half-maximum; MOPS, 3-(*N*-morpholino)propanesulfonic acid; Pc, plastocyanin; PS, photosystem; P700, reaction center chlorophyll of photosystem I.

0006-2960/96/0435-1282$12.00/0

The reaction between reduced Pc and $P700^+$ induced by short flashes has been studied in intact chloroplasts, stroma membranes, and isolated PSI particles (Haehnel et al., 1980, 1989, 1994; Olsen & Cox, 1982; Bottin & Mathis, 1985, 1987; Nordling et al., 1991; Sigfridsson et al., 1995). The time course of $P700^+$ reduction shows two dominant kinetic components, a fast one and a slower one (Haehnel et al., 1971). The fast component with a half-life of 11 μs is attributed to the first-order electron transfer within a complex between Pc and PSI (Haehnel et al., 1980). This electron transfer has been partially reconstituted with isolated PSI (Bottin and Mathis, 1985). Chemical cross-linking of Pc to PSI particles (Wynn & Malkin, 1988) has been shown to stabilize the active electron transfer complex by stoichiometric binding of Pc to subunit PsaF (Hippler et al., 1989). The half-life of the slow component was found to decrease at increasing concentrations of Pc and is attributed to the bimolecular reaction between soluble Pc and PSI. These findings could be rationalized by a reduction of $P700^+$ after formation of a complex between Pc and PSI in equilibrium with soluble Pc. However, Bottin and Mathis (1985) have proposed an additional intermediate bound state to account for the lower limit of 110 μs found for the half-life of the slow component at high concentrations of Pc. Complex kinetics of the electron transfer from Pc to P700 in subsequent flashes were suggested to indicate also that a reduced Pc bound to a second site transfers an electron to $P700^+$ bypassing or *via* the oxidized Pc occupying the first binding site (Bottin & Mathis, 1987).

In contrast to the binding of reduced Pc to PSI, the binding of oxidized Pc has received almost no attention. Therefore, we have first analyzed the interaction between reduced Pc and PSI particles in detail, providing the basis for a quantitative investigation of the reactions of oxidized Pc. We present several experimental approaches to the binding properties of oxidized Pc. The results characterize the oxidizing site of PSI on the basis of individual dissociation and rate constants for the oxidized and the reduced form of Pc. The values are consistent with an increased redox midpoint potential of Pc found in the bound state. The driving force of the electron transfer between Pc and P700 within the complex is derived. The release of oxidized Pc from the complex is resolved, and whether this release has to precede the binding of another reduced Pc in a subsequent turnover has been studied.

EXPERIMENTAL PROCEDURES

Preparation of Materials. PSI particles (PSI-200) were isolated from spinach leaves following the procedure of Wynn and Malkin (1988). Chlorophyll (Chl) concentrations were determined as described by Porra et al. (1989). The concentration of P700 was determined from laser-induced absorbance changes at 704 nm where the amplitude was 80% of that at the maximum of the difference spectrum at 701 nm (not shown). At the maximum we assumed an absorbance coefficient of 64 mM^{-1} cm^{-1} (Hiyama & Ke, 1972). PSI particles contained between 250 and 150 Chl per P700 and a molar ratio of Chl a/Chl b between 3.2 and >10, respectively. The values are given for each preparation of PSI particles. Pc was isolated from spinach leaves as described (Ratajczak et al., 1988). For stock solutions of fully oxidized or reduced Pc, ferricyanide or ascorbate was added, respectively, and then separated by gel filtration (PD10 columns, Pharmacia). The purified Pc in the oxidized or in the reduced state was used immediately for kinetic measurements, although no change of the oxidation state was observed during several hours at 0 °C. The concentration of Pc and degree of oxidation was determined spectroscopically using an extinction coefficient of 4.9 mM^{-1} cm^{-1} at 597 nm for the oxidized form (Katoh et al., 1962). Pc was cross-linked to PSI with ethylenediaminecarbodiimide (EDC) as described (Hippler et al., 1989) except that a pH value of 6.5 was adjusted with 30 mM 3-(*N*-morpholino)propanesulfonic acid (MOPS) buffer.

Kinetic Measurements. The standard reaction mixture contained PSI particles at a concentration of 95 μg of Chl/mL, 20 mM MOPS buffer (pH 7.0), 5 mM $MgCl_2$, 0.05% Triton X-100, 1 mM sodium ascorbate, 0.2 mM methyl viologen, 0.1 mM diaminodurene (DAD), and Pc as indicated. When oxidized and reduced Pc were added separately in defined stoichiometry, ascorbate and DAD were omitted. The oxidation state of Pc in these samples was determined spectroscopically after the kinetic measurements. A slight increase of the concentration of oxidized Pc by less than 5 μM was found, which is consistent with the number of flashes applied in the experiment. The absorbance changes of P700 were measured on a single-beam spectrophotometer essentially as described by Haehnel et al. (1994). The measuring light of 704 nm with 2.7 nm full width at half-maximum (FWHM) was switched on by opening of a photoshutter 5 ms before the recording was started. The cuvette containing 0.3 mL of the sample had an effective optical path length of 1.2 mm. The detecting photodiode (1 cm^2) was placed at a distance of 35 cm from the cuvette and protected by an interference filter of 704 nm. The output of the photodiode was amplified with an electrical bandwidth ranging from dc to 1 MHz with dc offset compensation by a combination of 16 bit analog to digital conversion (ADC) and a 16 bit digital to analog conversion (DAC) within 4 μs immediately before the recording. Flash excitation was from a frequency-doubled Nd:YAG laser (5 ns FWHM). For excitation by a second flash applied between 50 μs and 10 ms after the first flash a Xenon flash lamp was used (2 μs FWHM). Signal disturbance by fluorescence was monitored without measuring light and subtracted when necessary.

Redox Potentiometry. Redox titrations (Dutton & Wilson, 1974) were carried out with a 4 mL sample under argon in a cuvette with an optical path length of 10 mm. The following redox mediators were used: *p*-benzoquinone and *N*,*N*,*N*′,*N*′-tetramethyl-*p*-phenylenediamine at 5 μM, ferro- and ferricyanide at 10 μM. The ambient redox potential was varied by additions of ferricyanide or ascorbate. For measurement of the redox potential a platinum electrode and a Ag/AgCl reference electrode (saturated KCl) were used. The reference electrode was calibrated with solutions of quinhydrone at different pH at 25 °C. Redox potentials *versus* the standard hydrogen electrode were obtained according to Clark (1960).

Analysis of Kinetic Measurements. In a first evaluation absorption transients were fitted to a sum of two or three exponential components using Marquardt's least-squares fit algorithm. For the fast kinetic component the mean value of the half-life found at large amplitudes was kept constant in the curve-fitting of signals belonging to the same set of experiments but with a small amplitude, *e.g.*, at low concentrations of Pc and at high redox potentials, to improve the accuracy of the amplitude. A minor very slow component with a half-life in the range of 0.1 s did not depend

systematically on the Pc concentration. For the analysis of the two Pc dependent kinetic components the parameters of this component were kept constant at a mean value found in unrestricted fits. The half-lives of the fast and the slower components, $t_{1/2}(1)$ and $t_{1/2}(2)$, respectively, and the relative amplitude of the fast component $A(1)/[A(1)+A(2)]$ have been used by Nordling et al. (1991) to estimate the rate constant for binding of Pc^I to $P700^+$, $\bar{k}_{on}^I$, for the dissociation of the complex $\bar{k}_{off}^I$, and the intracomplex electron transfer, k_{et}, based on the model, $Pc^I + P700^+ \rightleftarrows Pc^I{\cdot}P700^+ \rightarrow Pc^{II}{\cdot}P700$. (In this paper we will use superscripts I and II to indicate reduced and oxidized Pc, respectively, and + to indicate PSI with oxidized P700.) The authors assumed (i) that the concentration of reduced Pc remains constant, *i.e.*, $[Pc^I] \gg [P700_{tot}]$ and implicitly presumed (ii) that there was no back electron transfer from reduced P700 to Pc^{II} and (iii) that oxidation of P700 did not change the rate constants of Pc. For this case the differential equations can be solved and explicit equations can be derived (Drepper, 1994) to estimate the rate constants $\bar{k}_{on}^I$, $\bar{k}_{off}^I$ and k_{et} from the amplitudes and half-lives [$\tau_i = t_{1/2}(i)/\ln 2$] by simple arithmetic operations

$$\bar{k}_{on}^{\ I} = \frac{(\tau_1\tau_2[Pc])^{-1}}{\tau_1^{-1} + \tau_2^{-1} - \left[\tau_1 + \frac{A(1)}{A(1)+A(2)}(\tau_2 - \tau_1)\right]^{-1}} \quad (1)$$

$$\bar{k}_{off}^{\ I} = \left[\tau_1 + \frac{A(1)}{A(1)+A(2)}(\tau_2 - \tau_1)\right]^{-1} - \bar{k}_{on}^{\ I}[Pc] \quad (2)$$

$$k_{et} = (\tau_1\tau_2\bar{k}_{on}^{\ I}[Pc])^{-1} \quad (3)$$

For simulations the concentration of individual species as a function of time was iteratively calculated from a set of rate equations by a fourth-order Runge−Kutta algorithm with a step width of 0.01 μs. Initial concentrations and first- and second-order rate constants are given in the figure legends. In a final analysis the time course of $P700^+$ reduction was fitted to the output of the numerical integration using Marquardt's algorithm. A restricted subset of the initial concentrations and rate constants was varied during the curve fitting procedure. The remaining "dependent" parameters were calculated for each subset of parameters from equations of restraints as given in the text. The restraints allowed inclusion of additional information into the numerical simulation, *e.g.*, an equilibrium constant determined from independent experiments.

RESULTS

Electron Transfer and Complex Formation between Plastocyanin and Photosystem I. Figure 1 shows the kinetics of P700 at 704 nm induced by a laser flash in PSI particles in the presence of soluble Pc. After oxidation in the flash the time course of $P700^+$ reduction can be deconvoluted into three distinct kinetic components. A fast component with an invariant half-life of 11 ± 1 μs at 25 °C, an intermediate or slower component with an amplitude $A(2)$, and a very slow component not greater than 5%−10% of the total signal which is shown by the extrapolated dotted lines in Figure 1. The latter component is almost not affected by Pc and seems to originate from a small fraction of PSI with very limited

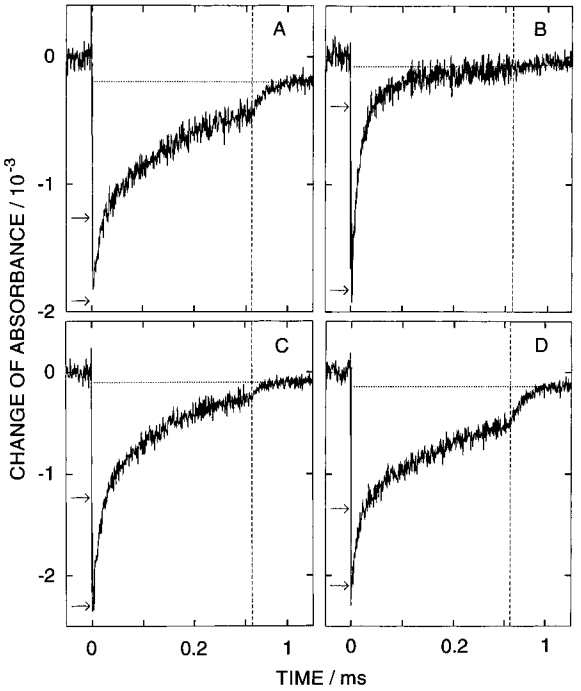

FIGURE 1: Absorbance changes at 704 nm induced by a laser flash in PSI particles in the presence of soluble plastocyanin. Reduced Pc was present at a concentration of 27 μM in A, 250 μM in B, 54 μM in C, and 54 μM *plus* oxidized Pc of 196 μM in D. The cuvette contained PSI particles at 95 μg of Chl/mL (Chl *a*/Chl *b* of 4.3), 5 mM $MgCl_2$, 30 mM MOPS pH 7.0, 0.05% Triton X-100, and 0.2 mM methyl viologen. Five individual signals were averaged for each trace at a repetition rate of 0.5 Hz. The time base was switched from 0.2 to 2 μs/address at 0.31 ms after the flash as marked by the dashed vertical line. The dotted horizontal line indicates the amplitude of the slow component. The amplitudes of the two exponential components fitted to the reduction kinetics of $P700^+$ are indicated by the two arrows. Their values and the half-lives are as follows: A, $\Delta A(1) = -0.65$, $t_{1/2}(1) = 11$ μs, $\Delta A(2) = -1.07$, $t_{1/2}(2) = 143$ μs; B, $\Delta A(1) = -1.44$, $t_{1/2}(1) = 11$ μs, $\Delta A(2) = -0.31$, $t_{1/2}(2) = 81$ μs; C, $\Delta A(1) = -1.10$, $t_{1/2}(1) = 10$ μs, $\Delta A(2) = -1.13$, $t_{1/2}(2) = 105$ μs; D, $\Delta A(1) = -0.76$, $t_{1/2}(1) = 10$ μs, $\Delta A(2) = -1.20$, $t_{1/2}(2) = 188$ μs.

reactivity. Therefore we have based our analysis on P700 accessible to Pc as represented by the two kinetic components, $A(1)$ and $A(2)$. Figure 1A,B shows that an increase of the concentration of reduced Pc from 27 to 250 μM increases the amplitude of the fast component $A(1)$ at the expense of the slower one $A(2)$. At the same time the half-life of the slower component decreases as it is known for second-order reactions. Figure 1C,D shows that addition of an excess of 196 μM oxidized Pc to 54 μM reduced Pc decreases $A(1)$ and increases the half-life of the slow component. For a quantitative approach we will first analyze the effect of reduced Pc.

Equilibrium of Complex Formation between Reduced Plastocyanin and Photosystem I. The concentration of active PSI without bound Pc, [P700] (for the sake of simplicity P700 will be used instead of PSI), and that of the complex, $[Pc^I{\cdot}P700]$, in the dark is related to the dissociation constant K_D^I

$$K_D^{\ I} = \frac{[Pc^I][P700]}{[Pc^I{\cdot}P700]} \quad (4)$$

The concentration of total P700, $[P700_{tot}]$, is given by the sum $[P700_{tot}] = [P700] + [Pc^I{\cdot}P700]$. By replacing [P700] with $[p700_{tot}] - [Pc^I{\cdot}P700]$, eq 4 can be rearranged to

describe the equilibrium at a concentration of reduced Pc, [Pc^I], in the dark before the flash,

$$\frac{[Pc^I][P700_{tot}]}{[Pc^I{\cdot}P700]} = [Pc^I] + K_D{}^I \quad (5)$$

However, the redox state of the components in the complex changes in the following ways: (i) The flash of saturating intensity at $t = 0$ oxidizes P700 and converts the complex $Pc^I{\cdot}P700$ to $Pc^I{\cdot}P700^+$. (ii) The redox potentials of Pc and P700 should not allow a complete electron transfer from Pc^I to $P700^+$ in the complex. The turnover may be limited by the equilibrium. If we include this effect in an empirical factor f ($f < 1$), then the relative amplitude $A(1)/A_{tot}$ observed after the flash is related to the fraction of the reduced complex before the flash by

$$\frac{A(1)}{A_{tot}} = f\frac{[Pc^I{\cdot}P700]}{[P700_{tot}]} \quad (6)$$

Combining eqs 5 and 6 yields eq 7

$$\frac{[Pc^I]}{A(1)/A_{tot}} = \frac{1}{f}[Pc^I] + \frac{K_D{}^I}{f} \quad (7)$$

which shows that a plot of [Pc^I] over the relative amplitude $A(1)/A_{tot}$ as a function of the concentration of Pc^I should indicate $1/f$ as the slope of the linear dependence and $-K_D{}^I$ as the intercept of the abscissa. This type of plot in Figure 2A shows a straight line for different batches of PSI particles. The value of the slope is within a narrow range between 1.1 and 1.2. By contrast the value of the intercept of the abscissa indicates a rather wide range of $K_D{}^I$. We have compared different preparations of PSI particles (not shown) and found extreme values of 7−10 and 60−70 μM for PSI particles with a molar ratio of Chl *a*/Chl *b* of about 9−10 and 3.5, respectively.

Binding of Reduced Plastocyanin to PSI with P700$^+$. The kinetic component $A(2)$ follows an exponential time course because the concentration of Pc^I exceeds that of P700 by more than 2 orders of magnitude. A second-order rate constant k_2 with values of $(1-4) \times 10^8$ M^{-1} s^{-1} may be estimated from the half-life $t_{1/2}(2)$ at concentrations lower than 5 μM Pc^I by $k_2 = \ln 2/(t_{1/2}(2)[Pc^I])$. However, the reduction of $P700^+$ in the fraction of PSI without bound Pc involves in addition to the bimolecular binding of Pc to PSI with $P700^+$ at least the electron transfer to $P700^+$ in the complex (*cf.* Experimental Procedures). Thus, at very high concentrations of reduced Pc the half-life should approach a limiting value. Therefore in Figure 2B the half-life is shown as a function of 1/[Pc^I]. The data can be fitted to a straight line. The intercept of the ordinate indicates a limiting half-life for all batches of PSI particles of 50−60 μs. This is considerably greater than 11 μs, *i.e.*, the half-life of the intracomplex electron transfer. However, it is important to note that at high Pc concentrations the amount of free P700 and the amplitude $A(2)$ approach zero, and the attribution of this half-life needs a detailed discussion (see below). The negative intercept of the abscissa, *i.e.*, the concentration at half of the minimal half-life, in Figure 2B shows a value of

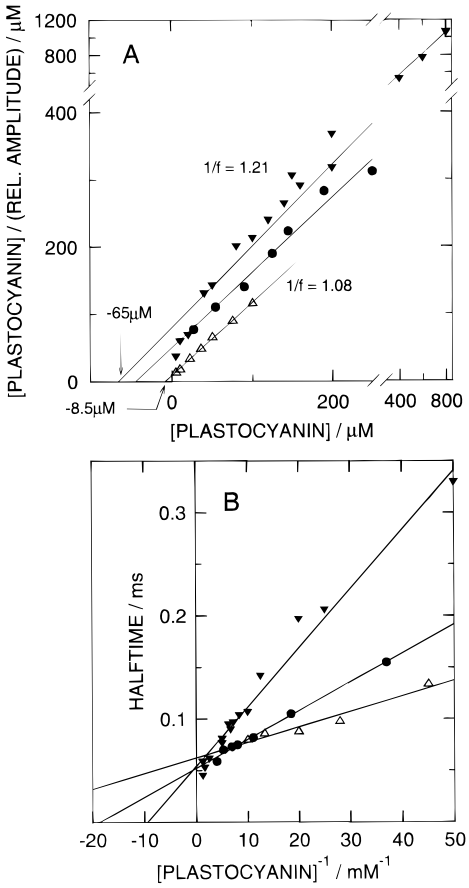

FIGURE 2: A: Amplitude of the fast kinetic component of $P700^+$ reduction as a function of the concentration of Pc in a reciprocal plot. Measurements using different batches of PSI particles are given by different symbols. The slope of the linear regression line and its intercept of the abscissa are as follows: ▼, 1.21 and −65 μM (Chl *a*/Chl *b* = 3.2); ●, 1.12 and −42 μM (Chl *a*/Chl *b* = 4.3); △, 1.08 and −8.5 μM (Chl *a*/Chl *b* = 10), respectively. B: Reciprocal pseudo-first-order rate of the slow component as a function of the reciprocal value of the plastocyanin concentration. Intercepts of the extrapolated straight lines through the data points with the vertical and with the horizontal axis are as follows: ▼, 54 μs and −106 μM; ●, 50 μs and −53 μM; △, 62 μs and −24 μM, respectively (same symbols as in A).

the same order of magnitude as the dissociation constant determined from the fast amplitude $A(1)$ for each of the PSI particles in Figure 2A.

Competitive Binding of Oxidized and Reduced Plastocyanin to Photosystem I. For a quantitative analysis of the effect of oxidized Pc on the reduction of $P700^+$ by Pc^I as shown in Figure 1C,D, we have to consider its competitive binding to PSI. The concentration of the complex with oxidized Pc, [$Pc^{II}{\cdot}P700$], is determined by its dissociation constant $K_D{}^{II}$ (*cf.* eq 4)

$$K_D{}^{II} = \frac{[Pc^{II}][P700]}{[Pc^{II}{\cdot}P700]} \quad (8)$$

A flash will create $Pc^{II}{\cdot}P700^+$, which does not contribute to the fast component of $P700^+$ reduction. However, $K_D{}^{II}$ can be determined from the decrease of the amplitude of the fast component. In the presence of Pc^{II} the concentration of total reduced P700 is given by the sum $[P700_{tot}] = [P700] + [Pc^I{\cdot}P700] + [Pc^{II}{\cdot}P700]$. Replacing [$Pc^{II}{\cdot}P700$], [P700], and $[P700_{tot}]/[Pc^I{\cdot}P700]$ by eqs 8, 4, and 6, respectively, and rearranging the result yields $K_D{}^{II}$ as a function of the relative

amplitude $A(1)/A_{tot}$ in the presence of $[Pc^{II}]$,

$$K_D{}^{II} = \frac{[Pc^{II}]}{\frac{[Pc^{I}]}{K_D{}^{I}}\left(\frac{f}{A(1)/A_{tot}} - 1\right) - 1} \quad (9)$$

Thus, with the values for $1/f$ and $K_D{}^{I}$ of 1.12 and 42 μM, respectively, taken from the plot of measurements in Figure 2A (closed circles), and the value of 0.39 for $A(1)/A_{tot}$ found with the same batch of PSI particles (with a low Chl *a*/Chl *b* ratio of 4.3) in the presence of 54 and 196 μM Pc^{I} and Pc^{II}, respectively, in Figure 1D, we estimate from eq 9 a value of 297 μM for $K_D{}^{II}$. A second measurement with these PSI particles (not shown) in the presence of 125 μM oxidized and 125 μM reduced Pc showed a relative amplitude $A(1)/A_{tot}$ of 57% as compared to 65% in the absence of oxidized Pc. The resulting value of $K_D{}^{II}$ is 185 μM, and the average of the two is 240 μM. The ratio of the dissociation constants $K_D{}^{II}/K_D{}^{I}$ is 5.7 for these PSI particles. A more precise determination has been carried out with a different batch of PSI particles. Figure 3A (diamonds) shows the amplitude of the 11 μs component as a function of reduced and oxidized Pc at a constant concentration of total Pc. For comparison the relative amplitude $A(1)/A_{tot}$ in the absence of oxidized Pc (*cf.* Figure 2A) is shown by circles and squares. The dashed line is equivalent to the linear fit in Figure 2A with a value of 8.5 μM for $K_D{}^{I}$. The solid line gives the fit of the data in the presence of reduced plus oxidized Pc to eq 9. As a result a value of 45 μM is found for $K_D{}^{II}$, which is 5.4 times higher than that of $K_D{}^{I}$.

Binding of Oxidized Plastocyanin to Photosystem I with Oxidized P700. Comparison of Figure 1C,D shows that oxidized Pc decreases also the rate of the slow Pc dependent component of $P700^+$ reduction. Different from the amplitude of the fast component, which probes the binding of Pc to PSI in the dark prior to the flash, *i.e.*, when P700 is reduced, the rate of the slow component should reflect the binding of Pc to PSI with oxidized $P700^+$ after the flash. If the binding of Pc^{II} to PSI reaches the equilibrium more quickly than the second-order binding of Pc^{I}, *i.e.*, for high excess of Pc^{II} over Pc^{I}, the slow kinetic component includes $P700^+$ and $Pc^{II}\cdot P700^+$, and the relative amplitude $A(2)/A_{tot}$ is given by $A(2)/A_{tot} = ([P700^+] + [Pc^{II}\cdot P700^+])/[P700_{tot}]$. Within this approximation $[Pc^{II}\cdot P700^+]$ can be substituted by the dissociation equilibrium of Pc^{II} and $P700^+$ with a constant $K_D{}^{II,+}$ (*cf.* eq 8).

$$\frac{A(2)}{A_{tot}} = \frac{[P700^+]}{[P700_{tot}]}\left(1 + \frac{[Pc^{II}]}{K_D{}^{II,+}}\right) \quad (10)$$

However, the electron transfer rate is determined by $[P700^+]$ alone because $Pc^{II}\cdot P700^+$ cannot accept electrons from Pc^{I}, $dA(2)/dt = k_2[P700^+][Pc^{I}]$. By replacing $[P700^+]$ with eq 10 the integration shows that the half-life in the absence and presence of oxidized Pc at a concentration $[Pc^{II}]$, $t_{1/2}$ and $t_{1/2}{}^{II}$, respectively, can be used to determine $K_D{}^{II,+}$ by eq 11

$$K_D{}^{II,+} = [Pc^{II}]\frac{t_{1/2}}{at_{1/2}{}^{II} - t_{1/2}} \quad (11)$$

where *a* is the ratio of $[Pc^{I}]$ in the presence over that in the absence of Pc^{II}, *i.e.*, *a* equals 1 if $[Pc^{I}]$ is the same in both experiments. The slow component of the kinetics in Figure 1C,D with a half-life of 105 and 188 μs, respectively, indicates $K_D{}^{II,+} = 250$ μM. The value appears to be slightly higher than that of $K_D{}^{II}$. This has been examined in more detail. Figure 3B presents the effect of oxidized Pc on the reciprocal half-life of the slow component in PSI particles with a high Chl *a*/Chl *b* ratio of 10. The full circles and the dashed line give the data and the regression line, respectively, from Figure 2B as reference. Equation 11 is used to calculate relative to this line the best fit to the measurements in the presence of Pc^{II} (diamonds), yielding a value of 80 μM for $K_D{}^{II,+}$. This shows more clearly that the value of $K_D{}^{II,+}$ is about 2-fold higher than that of $K_D{}^{II}$ of 45 μM in Figure 3A. Although still an approximation, the result indicates a decrease of the binding affinity of oxidized Pc to PSI when

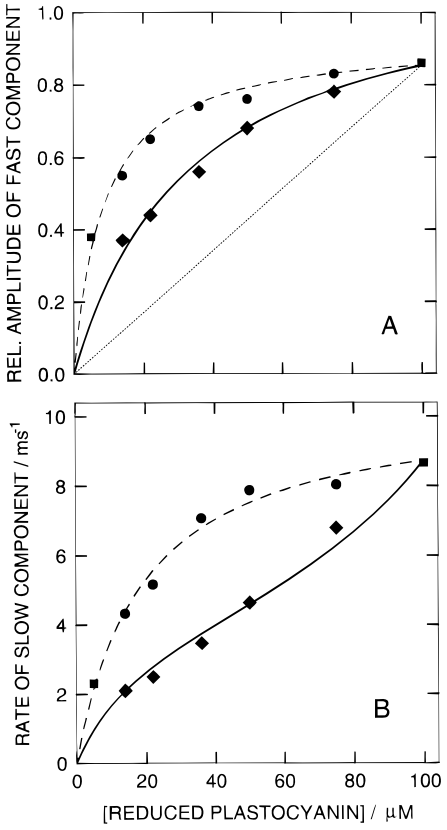

FIGURE 3: Effect of oxidized Pc on the reactions between reduced Pc and PSI. A: Amplitude of the 11 μs component as a function of the concentration of reduced Pc in the absence (circles and squares) and in the presence (diamonds) of oxidized Pc for PSI particles with Chl *a*/Chl *b* = 10. The total concentration of Pc ($[Pc^{II}] + [Pc^{I}]$) in the experiments given by diamonds was 100 μM. Only in experiments given by squares were 1 mM ascorbate and 0.1 mM DAD present. Other conditions are as in Figure 1. To the data points in the absence of oxidized Pc, eq 7 was fitted (dashed line) with values for $K_D{}^{I}$ and *f* of 8.5 μM and 0.93, respectively. The solid line is calculated from the dashed line and eq 9 with $K_D{}^{II} = 45$ μM to estimate the amount of complex between PSI and Pc^{I} in the presence of Pc^{II}. The dotted line indicates where the data points would be expected in the presence of Pc^{II} if the dissociation constants of oxidized and reduced Pc were equal (at a constant total concentration of Pc). B: Rate constant of the slow kinetic component as a function of the concentration of reduced Pc in the absence (circles, squares) and in the presence of oxidized Pc (diamonds) for the same experiments as in A. The dashed line represents a fit to the data points in the absence of Pc^{II} and corresponds to the linear regression in Figure 2B (open triangles). The solid line is the fit of eq 11 to the data in the presence of Pc^{II} yielding a value for $K_D{}^{II,+}$ of 80 μM, taking into account the fit by the dashed line.

P700 becomes photooxidized.

Redox Potential of Bound Plastocyanin. A different dissociation constant of the reduced and the oxidized forms of a molecule indicates a difference between the midpoint redox potential of the molecule in the free and the bound state [*cf.* Moser and Dutton (1988)]. The oxidation−reduction equilibrium of Pc in solution at an ambient redox potential E_h is described by Nernst's equation ($T = 298$ K)

$$E_h = E_m^{fr} + 59mV \log\left(\frac{[Pc^{II}]}{[Pc^{I}]}\right) \qquad (12a)$$

where E_m^{fr} denotes the midpoint potential of free Pc. An analogous equation can be written for Pc bound to PSI with a midpoint potential E_m^{bd}.

$$E_h = E_m^{bd} + 59mV \log\left(\frac{[Pc^{II}\cdot P700]}{[Pc^{I}\cdot P700]}\right) \qquad (12b)$$

In a common system E_h in eqs 12a,b is equal. Replacing the concentrations by eqs 4 and 8 shows that the difference of the midpoint potential in the bound and the free states is related to the ratio of the dissociation constants by eq 13.

$$E_m^{bd} - E_m^{fr} = 59mV \log\left(\frac{K_D^{II}}{K_D^{I}}\right) \qquad (13)$$

Our first approximation to the ratio of the dissociation constants of about 5.4−5.7 suggests an increase of the midpoint potential by 43−45 mV of bound relative to free Pc, independent of the type of PSI particles. Therefore, the effect of the redox potential has been studied in detail.

Effect of the Ambient Redox Potential on Electron Transfer from Soluble Pc to P700$^+$. The amount of bound Pc^I as a function of the redox potential was studied by monitoring $A(1)$. The result of such a redox titration in the presence of 40 μM Pc^I is shown in Figure 4A (circles). The data are fitted to Nernst's equation with an apparent midpoint potential E_m^{app} of 374 mV. Under the same conditions with respect to ionic strength and temperature the redox titration of Pc in solution yielded a midpoint potential E_m^{fr} of 360 mV (triangles in Figure 4A) which is close to values reported previously (Katoh et al., 1962; Sanderson et al., 1986; Armstrong et al., 1985). Thus, the apparent midpoint redox potential of the amplitude $A(1)$ of the fast component in the presence of 40 μM Pc is only slightly increased by 14 mV relative to that of free Pc in contrast to the expected increase by at least 45 mV. The redox titration was repeated in the presence of 400 μM Pc (Figure 4A, squares) which showed an apparent midpoint potential of 394 mV, *i.e.*, an increase of 34 mV. This effect of the concentration and the difference of the apparent midpoint potential from the value expected from the dissociation constants can be rationalized (see Discussion and Appendix).

Redox Titration of Plastocyanin Covalently Bound to PSI. Pc can be cross-linked with ethylenediaminocarbodiimide (EDC) to PSI competent in fast electron transfer (Hippler et al., 1989). Figure 4B shows the amplitude of the fast component and the total amplitude of the signal as a function of the redox potential. The inset of Figure 4B shows the absorbance change induced by a single laser flash at low redox potential after equilibration in the dark. The total amplitude gives the total amount of reduced P700 being

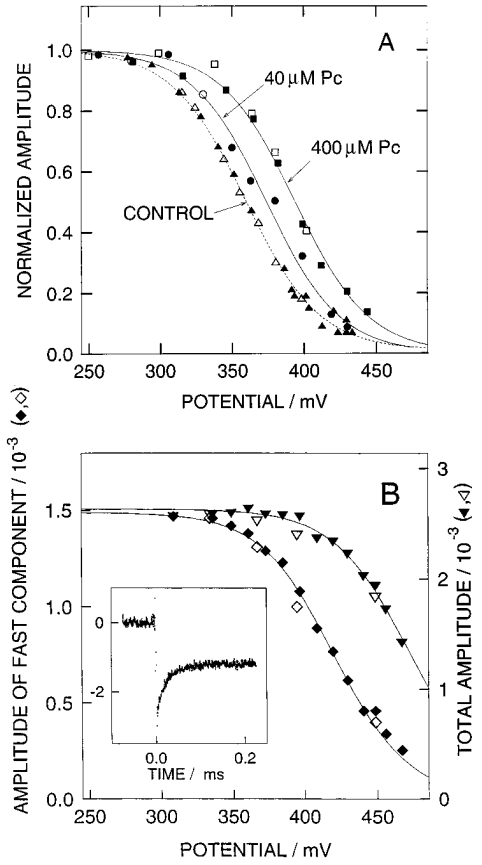

FIGURE 4: Effect of the ambient redox potential on the amplitude of the fast kinetic component of P700$^+$ reduction. A: Relative amplitude of the 11 μs component using PSI particles (Chl *a*/Chl *b* = 3.7) in the presence of 40 μM (●, ○) and 400 μM Pc (■, □). The maximal value normalized to 1 corresponds to relative amplitudes of 0.46 and 0.87 at 40 and 400 μM, respectively. Data points were fitted by Nernst's equation (solid lines) with a midpoint potential E_m^{app} of 374 and 394 mV, respectively. The redox titration of Pc in solution monitoring the absorbance at 597 nm as a function of the ambient redox potential is shown as control (▲, △) yielding $E_m^{fr} = 360$ mV. B: Amplitude of the fast component (◆, ◇) and total amplitude (▼, ▽) of P700$^+$ reduction kinetics using PSI particles with cross-linked Pc. Solid lines represent the fit of Nernst's equation to the data with E_m values of 421 and 475 mV, respectively. The inset shows an absorbance transient induced by a single laser flash at an ambient redox potential of 305 mV. Data from oxidative titrations are indicated by full, reductive titrations by open symbols.

oxidized by the flash. The amplitude of the fast reduction representing 60% of the total amplitude of the signal indicates the amount of PSI with Pc cross-linked in a functional complex. The half-life of 15 μs is close to 11 μs found with soluble Pc (*cf.* Figure 1). Fits to Nernst's equation indicate midpoint potentials of 421 and 475 mV for cross-linked Pc and P700 (diamonds and triangles in Figure 4B), respectively. The small difference in redox potential of ca. 55 mV limits the electron transfer from bound Pc^I to P700$^+$ to 89% of total reduced Pc and suggests from the relative amplitude of 0.60 that the fraction of PSI with cross-linked Pc was actually 67% of total PSI.

Release of Plastocyanin after Intracomplex Electron Transfer. An important aspect of the electron transfer mechanism is the question of whether oxidized Pc has to leave its binding site at PSI before a subsequent reduction of P700$^+$ can take place. Alternative mechanisms could be an electron transfer to P700$^+$ through the bound Pc molecule or from a second binding site at PSI. These possibilities have been investigated with Pc cross-linked to PSI particles.

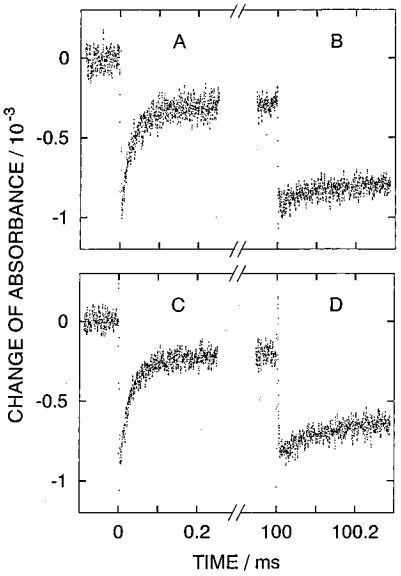

FIGURE 5: Absorbance changes of P700 induced by two laser flashes given at $t = 0$ and 100 ms using PSI particles with cross-linked Pc. Experiments in the absence (traces A and B) and in the presence of 70 μM reduced Pc (traces C and D). Experimental conditions as in Figure 1 except that 1 mM ascorbate and 2 μM diaminodurene were added. Ten signals were averaged at a repetition rate of 0.05 Hz.

Figure 5 shows the reduction kinetics of $P700^+$ induced after dark adaptation by two laser flashes at an interval of 100 ms in the absence (A and B) and presence (C and D) of soluble Pc. In Figure 5A, after the first flash 75% of total $P700^+$ is reduced with a half-life of 15 μs by the cross-linked Pc, *i.e.*, more than 80% of total PSI was cross-linked to an active Pc molecule in this preparation. After the second flash a small fraction of only 15% of total $P700^+$ is rapidly reduced (Figure 5B). This indicates a small fraction of bound Pc, which is reduced by ascorbate during the time interval between the flashes. Figure 5C,D shows the time course in the presence of 70 μM reduced soluble Pc. The two signals are almost identical to those in Figure 5A,B. In particular the signals after the second flash indicate that the reduction of $P700^+$ in the complex by soluble Pc in addition to the reduction by ascorbate is negligible during the time of 100 ms between the flashes. At the high concentration of 70 μM soluble Pc, $P700^+$ would be reduced with a half-life shorter than 100 μs (*cf.* Figure 1). Thus, when the binding site is occupied by oxidized Pc, the electron donation from Pc^I in solution to the complex in the states Pc^{II}•P700 and Pc^{II}•$P700^+$ as indicated by the amplitudes and the time course, respectively, in Figure 5D is orders of magnitude slower than that to $P700^+$ in PSI with a free Pc binding site. Thus, an electron transfer to the cross-linked complex *via* bound Pc or to P700 directly can be excluded.

Reactions of Oxidized Plastocyanin in the Complete Reaction Cycle. The result shown in Figure 5 emphasizes that the release of oxidized Pc from its binding site is an important step for a complete turnover in the reaction cycle of PSI. We have probed the release of the oxidized and the successive binding of soluble reduced Pc to PSI by a flash given at time intervals in the microsecond range after a preceding laser flash. After the first flash the fast component of $P700^+$ reduction was very similar to that in Figure 1B showing a half-life of 10 μs and a relative amplitude of $A(1)$ of 0.76 in the presence of 250 μM soluble reduced Pc.

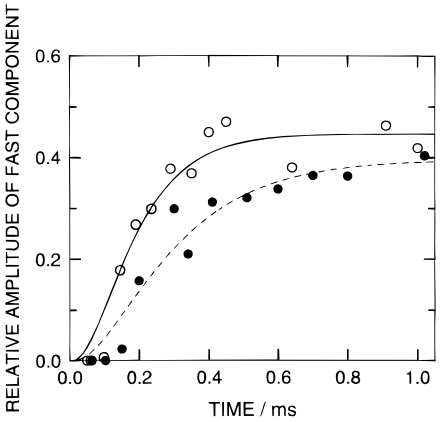

FIGURE 6: Relative amplitude of the fast kinetic component of $P700^+$ reduction following a second flash as a function of the time interval between the first and the second flash in the presence of 250 μM (open circles) and 100 μM (closed circles) reduced Pc. PSI particles at a concentration of 190 μg of Chl/mL (Chl *a*/Chl *b*: 3.1). Time courses calculated by analytical solution for the final product of three consecutive first-order reactions are shown (lines). For the best fit to the data points the following rate constants were used: $k_{et} = 53\ ms^{-1}$ [$t_{1/2}(1) = 13\ \mu s$], $k_{off}^{II} = 9.2\ ms^{-1}$, $k_{on}^{I} = 5 \times 10^7\ s^{-1}\ M^{-1}$. $k_{on}^{I}[Pc^I]$ was considered to be a pseudo-first-order rate constant at 250 μM (full line) and 100 μM (dashed line) Pc^I.

Figure 6 presents the relative amplitude of the fast component as a function of the time interval between the two flashes in the presence of soluble Pc. The time course shows a lag of about 50 and 60 μs and a rise with a half-life of 180 and 220 μs at 250 and 100 μM Pc^I, respectively. It is worth noting that during this lag time of 60 μs after the first flash, *i.e.*, after 6 half-lives, the oxidation of bound Pc^I is largely complete. However, after this time a fast component is not detected and the kinetics does not follow a first-order time course (not shown). Thus, oxidized Pc at the binding site has not been replaced by reduced Pc during this period of time. The exchange of the oxidized by a reduced Pc molecule at the binding site is monitored by the rising amplitude. The effect of the concentration indicates the contribution of a second-order reaction to this process. The time course should be dominated by three consecutive events: the first-order oxidation of bound Pc^I with a half-life of 10−11 μs, a first-order release of oxidized Pc^{II}, and a second-order binding of Pc^I with a pseudo-first-order time course

$$Pc^I\text{•}P700^+ \rightarrow Pc^{II}\text{•}P700 \rightarrow P700 \rightarrow Pc^I\text{•}P700$$

with rate constants k_{et}, k_{off}^{II}, and $k_{on}^{I}[Pc^I]$, respectively. Such a sequence of three first-order reactions has been integrated, *e.g.*, for the radioactive decay. Since k_{et} is known, k_{off}^{II} and k_{on}^{I} were fitted to the data points at the two concentrations of Pc^I by the explicit solution for the final product of three consecutive first-order reactions (lines in Figure 6), yielding estimates of $9.2 \times 10^3\ s^{-1}$ and $5 \times 10^7\ M^{-1}\ s^{-1}$, respectively. The value of k_{off}^{II} is three times higher than that of $\bar{k}_{off}^{I}$ of $3 \times 10^3\ s^{-1}$ estimated from the kinetics induced by the first flash and eqs 1−3. It should be mentioned that the amplitude of the fast component in Figure 6 after the second flash is about one-third smaller than that after the first flash. This is caused by double excitation of some PSI during the xenon flash with an intensity profile tailing as long as the half-life of the fast component. However, the fraction of $A(1)$ should be constant and the time course should not be disturbed.

Scheme 1: Model of the Binding Dynamics between Pc and PSI and Electron Transfer between the Cu Center of Pc and P700 within a Complex with a Single Binding Site[a]

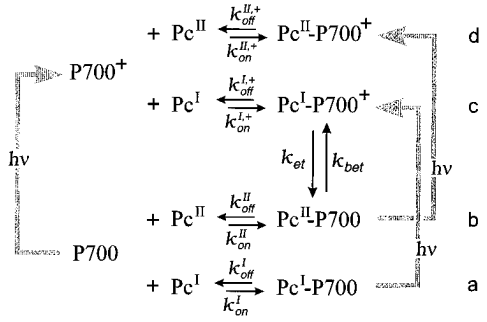

[a] A binding equilibrium between Pc and PSI is assumed with a second-order rate constant k_{on} for the formation and a first-order rate constant k_{off} for the dissociation of the "enzyme−substrate complex". Superscripts I and II indicate the participation of reduced and oxidized Pc, respectively, and superscript + indicates that of oxidized P700. A single-turnover flash converts the binding equilibria with reduced P700 (a, b) to those with the oxidized $P700^+$ (c, d). Subsequently, $P700^+$ re-reduction occurs within the "activated enzyme-substrate complex" $Pc^I{\cdot}P700^+$, yielding the "enzyme−product complex" $Pc^{II}{\cdot}P700$. The release of Pc^{II} with the rate constant k_{off}^{II} leads to the state P700 within the initial equilibrium (a). When oxidized Pc is present before the flash, the binding equilibrium between PSI and Pc^{II} has to be included (b). Under these conditions or if two flashes are given with a short interval the state $[Pc^{II}{\cdot}P700^+]$, a "product−inhibition complex" may be produced (d). For the sake of simplicity we do not explicitly give the differential equations used in the numerical simulations. But we refer to individual reactions of this scheme which can be directly translated into a set of linear differential equations.

DISCUSSION

The simplest and complete model of the electron transfer from the soluble protein Pc to the multiprotein complex of PSI includes the binding equilibrium between each of the species in its oxidized and reduced state and the equilibrium of the electron transfer reaction. Scheme 1 summarizes all individual reactions and gives the rate constants with indices as used in this paper (see Experimental Procedures). The binding equilibria are characterized by their dissociation constant $K_D = k_{off}/k_{on}$. A laser flash will convert reduced P700 in any state to $P700^+$, as indicated by the arrows labeled *hν*. To extend current knowledge about the dynamic interaction between the proteins, the investigations were focused on the following aspects: (i) the effect of the oxidation state of the two reaction partners on the dissociation constants of the complex; (ii) the midpoint redox potential of the bound reactants, Pc and P700, which determines the driving force of the electron transfer; (iii) the dynamics of the bound reaction product Pc^{II}; (iv) a quantitative description of the system by a complete set of differential equations. We have also derived equations which provide a reasonable approximation to the constants by standard methods of data analysis. The experimental approach can be summarized as follows: (i) The reactions between Pc and PSI with reduced or oxidized P700 are analyzed from the fast first-order and the slower second-order reaction, respectively. (ii) In both of these states the kinetic constants of oxidized Pc can be estimated from the competitive inhibition of the reactions with reduced Pc. (iii) Redox titrations are carried out to determine the equilibrium constant of the intracomplex electron transfer. (iv) The second flash of a double flash is used to study the reactions involved in the turnover of the complex. PSI preparations containing either pure PSI complexes or PSI associated with additional light-harvesting complexes or membrane fragments show differences in some of the kinetic parameters but not in the mechanism.

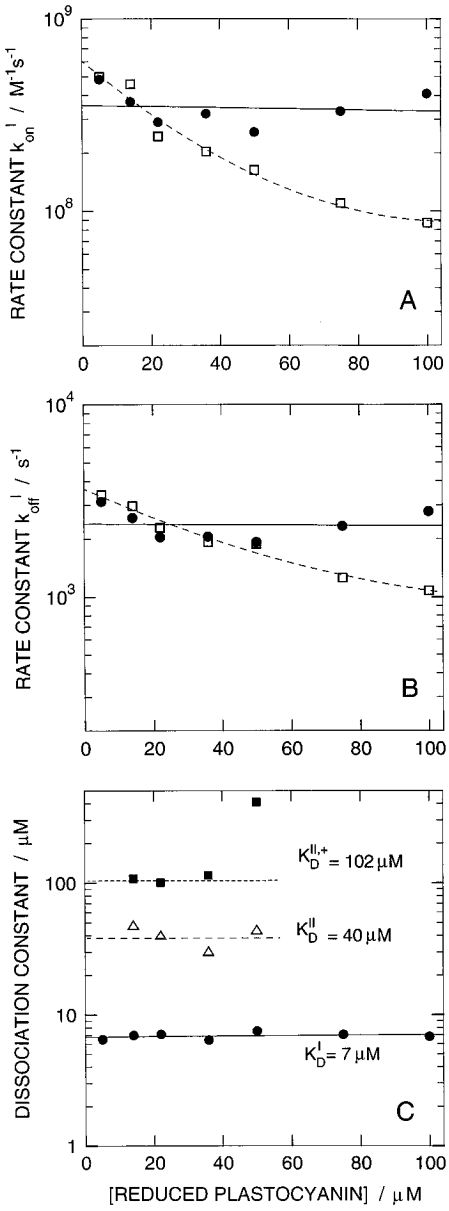

FIGURE 7: A, B: Rate constants $\bar{k}_{on}^I$ (A) and $\bar{k}_{off}^I$ (B) determined by the fit of $P700^+$ reduction kinetics to the numerical solution of differential equations according to Scheme 1 (filled symbols). The mean values for $\bar{k}_{on}^I$ and $\bar{k}_{off}^I$ are $(3.5 \pm 1) \times 10^8\ M^{-1}\ s^{-1}$ and $(2.4 \pm 0.5) \times 10^3\ s^{-1}$, respectively. Open symbols give the respective rate constants calculated from eqs 1 and 2 based on the two exponential fits for the same measurements shown by the open symbols in Figure 3. The values found by extrapolation to 0 μM reduced Pc are $6 \times 10^8\ M^{-1}\ s^{-1}$ and $3.7 \times 10^3\ s^{-1}$. C: Dissociation constants K_D^I (full circles, determined in the absence of Pc^{II}, *cf.* A and B), K_D^{II} and $K_D^{II,+}$ (open triangles and filled squares, respectively; $[Pc_{tot}] = 100\ \mu M$) in the presence of both oxidized and reduced Pc. Results from a fit of differential equations to the measurements shown by full symbols in Figure 3 (for further details see text).

Rate Constants for Reactions of Reduced Plastocyanin. The laser-induced reduction kinetics of $P700^+$ by Pc^I has been analyzed by a two-exponential fit on the basis of a simple equilibrium of complex formation (Nordling et al., 1991) as detailed above by eqs 1−3 (*cf.* Scheme 1c). The data shown in Figure 2 by open triangles have been used to calculate $\bar{k}_{on}^I$ and $\bar{k}_{off}^I$ from eqs 1 and 2. The values are shown for comparison by open squares in Figure 7A,B, respectively. These rate "constants" depend considerably on

the concentration of Pc^I. One reason for this discrepancy is the incomplete turnover of the complex as a consequence of the small redox potential difference of 55 mV in the complex (*i.e.*, $k_{bet} > 0$), not known previously. This effect of the concentration led us to reanalyze the time course of $P700^+$ in a more detailed approach including the dissociation of Pc^I ($k_{off}^{I,+}$, Scheme 1c) and of Pc^{II} (k_{off}^{II}, Scheme 1b), which compete with the forward (k_{et}) and backward (k_{bet}) electron transfer within the complex, respectively. Although the dissociation is complex, the binding of Pc^I is a single second-order step. Therefore extrapolation of the slow component of the two-exponential analysis to zero concentration of Pc^I, where the contribution of the bound state to the kinetics should be minimal, can be used as a good approximation to $k_{on}^{I,+}$ as verified by fits to numerical calculations using the complete model in Scheme 1 (not shown). $k_{on}^{I,+}$ shows a very high value of 6×10^8 M^{-1} s^{-1} in Figure 7A. For a more quantitative approach under reducing conditions we have to take into account as variable parameters the ratio of the initial concentrations, $[P700^+]_{t=0}/[Pc^I \cdot P700^+]_{t=0}$, and five rate constants, $k_{on}^{I,+}$, $k_{off}^{I,+}$, k_{et}, k_{bet}, and k_{off}^{II}. $[Pc^I]$ is assumed to be constant.

The number of independent variables can be reduced by the following restraints: (i) $k_{bet} = k_{et}/K_{eq}$. The equilibrium constant $K_{eq} = 10$ is determined from redox potentials (see also below). (ii) $k_{on}^I = k_{on}^{I,+}$ and $k_{off}^I = k_{off}^{I,+}$ (referred to as the average values $\bar{k}_{on}^I$ and $\bar{k}_{off}^I$, respectively). Arguments that the oxidation state of P700 may have a negligible effect on the binding constants of Pc^I will be discussed below. The value for $\bar{k}_{off}^I$ is derived from the ratio of the initial concentrations, $k_{off}^I = [P700^+]_{t=0}/[Pc^I \cdot P700^+]_{t=0} k_{on}^I [Pc^I]$ (*cf.* eq 4). (iii) k_{off}^{II} is determined from double-flash experiments (*cf.* Figure 6). During the calculations it is defined by the equation of restraint, $k_{off}^{II}/k_{off}^I = 2.8$. This ratio is in line with the difference between the midpoint redox potentials for free and bound Pc (Figure 4A,B) if equal contributions are assumed from on- and off-rates to the differences in the dissociation constants for Pc^I and Pc^{II} (*cf.* eq 13). The remaining three independent variables, *i.e.*, the ratio of initial concentrations $[P700^+]_{t=0}/[Pc^I \cdot P700^+]_{t=0}$ and the rate constants $\bar{k}_{on}^I$ and k_{et}, were determined from the fit of a numerical solution of the differential equations (representing the reactions in Scheme 1) to the time course of $P700^+$ reduction. The quality of the fits as judged from the computed sum of the squared residuals was generally equal or better than that with the fit of the sum of two exponentials. It is of note that the number of fitted parameters as well as the neglected effect of the oxidation state of P700 is the same as that used in the two-exponential fit by Nordling et al. (1991). Figure 7A,B (filled symbols) shows that the rate constants $\bar{k}_{on}^I$ and $\bar{k}_{off}^I$ determined by the fit of the differential equations give a consistent description of the experimental data at both low and high concentrations of Pc^I. The values of the rate constant $\bar{k}_{on}^I$ and $\bar{k}_{off}^I$ are $(3.5 \pm 0.8) \times 10^8$ M^{-1} s^{-1} and $(2.4 \pm 0.5) \times 10^3$ s^{-1}, respectively, for this batch of PSI particles. The ratio $\bar{k}_{off}^I / \bar{k}_{on}^I$ shows a constant value of 7 μM in Figure 7C, which is close to the value of 8.5 μM estimated for K_D^I in Figure 2A. For comparison the results of the numerical approach and the values from the approximating equations are summarized in Table 1.

Competitive Binding of Oxidized and Reduced Plastocyanin. An approximation to the dissociation constant K_D^{II} of

Table 1: Kinetic Parameters for Binding Dynamics and Electron Transfer between Pc and PSI for Two Typical Batches of PSI Particles and Midpoint Potentials of the Redox Cofactors[a]

PSI particles,[b] Chl *a*/Chl *b*	rate constant: Pc binding[c] (10^8 M^{-1} s^{-1})		rate constant: Pc release[d] (10^3 s^{-1})		dissociation constant (μM)			electron transfer[e] (10^3 s^{-1})		midpoint potentials (mV): $Pc(Cu^{II}/Cu^I)$		midpoint potentials (mV): $P700^+/P700$[f]	
	$\bar{k}_{on}^I$	k_{on}^{II}	$\bar{k}_{off}^I$	$\bar{k}_{off}^{II}$[g]	$\bar{K}_D^I$[h]	K_D^{II}	$K_D^{II,+}$	k_{et}	k_{bet}	E_m^{fr}	E_m^{bd}	E_m	$E_m(Pc^{II})$
4.3	1.1 ± 0.5	0.4 ± 0.2	3.2 ± 1	8 ± 2.5	≈ 13	29 ± 4 (42 ± 12)	190 ± 30 (240 ± 60)	(≈ 250)					
10	3.5 ± 1[i]	1.7 ± 0.4	2.4 ± 0.5	6.7 ± 1.4	11 ± 1.5	7 ± 0.7 (8.5 ± 1.5)	40 ± 6 (45 ± 10)	102 ± 15 (≈ 80)	58 ± 10	4.5 ± 1.5	360 ± 5	410 ± 10	475 ± 10	ca. 500

[a] Values in parenthesis have been estimated from the data in Figures 1−3 and eqs 7, 9, or 11. [b] Chl extinction coefficients from Porra et al. (1989). [c] Rate constants are the results from final analysis of $P700^+$ reduction kinetics using the set of differential equations representing all reactions in Scheme 1 (see Figure 7 and text for explanation). [d] The ratio k_{off}^{II}/k_{off}^I is determined from fit of kinetics after two flashes at different time intervals (see Figure 6). [e] k_{bet} is calculated from $k_{bet} = k_{et}/\exp(-\Delta G°/RT)$ using the midpoint potentials from equilibrium redox titrations. [f] E_m for $P700^+/P700$ without bound Pc is assumed to be equal to that in the presence of Pc^I. E_m in the presence of Pc^{II} is estimated from dissociation constants (see text). [g] The fit of the time course after double flashes in Figure 6 gives 9.2×10^3 s^{-1}, the limiting time of 60 μs in Figure 2B ca. 12×10^3 s^{-1}. [h] K_D^I from simulation of differential equations is based on the assumption $K_D^I = K_D^{I,+}$ (see text for more information). The values in brackets give K_D^I estimated as shown in Figure 2A. [i] Extrapolation in Figure 7A gives $k_{on}^{I,+} = 6 \times 10^8$ $M^{-1}s^{-1}$ as detailed in the text.

oxidized Pc bound to PSI with reduced P700 is given by eq 9. The approximation by eq 11 to the dissociation constant $K_D^{II,+}$ for Pc^{II} bound to PSI with oxidized P700 includes assumptions that suggest a reexamination of the first estimate. For a numerical solution of the differential equations simulating the $P700^+$ reduction after a flash in the presence of both oxidized and reduced Pc we have to include the initial concentration, $[Pc^{II}\cdot P700^+]_{t=0}$, and three rate constants, $k_{on}^{II,+}$, $k_{off}^{II,+}$, and k_{on}^{II} (*cf.* Scheme 1), in addition to the parameters summarized above. Therefore the rate constants $\bar{k}_{on}^{I}$, $\bar{k}_{off}^{I}$, and k_{et} have to be determined in the absence of Pc^{II}. In addition to the restraints i−iii, we use the equation (iv) $k_{on}^{II} = k_{off}^{II}[Pc^{II}\cdot P700^+]_{t=0}/([P700^+]_{t=0}[Pc^{II}])$ and the assumption (v) $k_{off}^{II} = Ck_{off}^{II,+}$, in which the constant C is initially set to 1 (*i.e.*, $\bar{k}_{off}^{II}$). However, $k_{on}^{II,+}$ and k_{on}^{II} are not set equal to test an effect of the P700 oxidation state on the binding of Pc^{II}. The values derived from the fit are included in Table 1. The difference between the two values indicates different dissociation constants of the two respective complexes. It is attributed to equal contributions from the on- and off-rates of Pc^{II} to the dissociation constants K_D^{II} and $K_D^{II,+}$, *i.e.*, $k_{on}^{II,+}/k_{on}^{II} = C = k_{off}^{II}/k_{off}^{II,+}$. Figure 7C summarizes the dissociation constants derived from the measurements shown by filled symbols in Figure 3 and shows values of 40 and 102 μM for K_D^{II} and $K_D^{II,+}$, respectively. Only at concentrations of $[Pc^{II}] > [Pc^{I}]$ did the fit of the differential equations converge. The value of K_D^{II}/K_D^{I} of 5.7 is very similar to 5.4 found with the approximation by eq 9 in Figure 3. The value of the constant $K_D^{II,+}$ of 102 μM exceeds that of 80 μM determined from Figure 3B. The result is in support of eq 11 being a reasonable approximation.

Binding Equilibria and Shift in Redox Potential of Plastocyanin. The higher value of the dissociation constant K_D^{II} than that of K_D^{I} indicates a preferential binding of reduced Pc to PSI. As a consequence the midpoint potential is predicted to be increased by 45 mV relative to that of free Pc, *cf.* eq 13. The midpoint potential of 420 mV of Pc functionally cross-linked to PSI particles shows a slightly larger increase of 60 mV relative to free Pc. A minor shift of the redox potential by a conformational distortion of the cross-linked complex as compared to the native one may be possible.

In solution the data in Figure 4A indicate an apparent midpoint potential of the fast amplitude of only 374 and 394 mV in the presence of 40 and 400 μM Pc, respectively. This effect of the concentration can be understood because the amplitude of the fast component $A(1)$ monitors only $Pc^{I}\cdot$ P700 but not $Pc^{II}\cdot$P700 as discussed for eqs 6 and 9. The apparent midpoint potential E_m^{app} of the titrations in Figure 4A gives the redox potential at which the amount of bound Pc^{I} is half of its maximal amount. With respect to the ratio K_D^{II}/K_D^{I} of 5.7 the amount of bound Pc^{II} must be significantly lower than that of Pc^{I}. The true midpoint potential of bound Pc in eq 12b, given when $[Pc^{I}\cdot P700]$ equals $[Pc^{II}\cdot P700]$, must be higher than the apparent one. This effect would be negligible when all binding sites at PSI are saturated at high concentrations of Pc. The analysis of the reduced complex $Pc^{I}\cdot$P700 as a function of the redox potential has to take into account the dissociation constants K_D^{I} and K_D^{II} as well as the concentration of total Pc $[Pc_{tot}]$. The redox potential E_m^{app} can be related to the true midpoint potential of bound Pc, E_m^{bd}, using eqs 4, 8, and 13 and is given by eq 14 (for a derivation see Appendix).

$$E_m^{app} = E_m^{bd} - 59mV \log\left(\frac{K_D^{II} + [Pc_{tot}]}{K_D^{I} + [Pc_{tot}]}\right) \qquad (14)$$

E_m^{bd} is estimated to be about 405 mV from both of the experimental values of E_m^{app} in Figure 4A, the respective total concentration of Pc and the values of 42 (*cf.* Figure 2A) and 240 μM found for K_D^{I} and K_D^{II}, respectively, with this batch of PSI particles. Thus, the three independent approaches give a consistent result for the dissociation constants and the shift of the redox potential of bound Pc not only in the cross-linked state but also in dynamic binding equilibrium. Possible conformational distortions of the cross-linked as compared to the native complex cannot be large.

A midpoint potential of 385 mV was found for the amplitude of the fast component of $P700^+$ reduction in pea chloroplasts (Bottin & Mathis, 1985). The attribution of this value to the E_m of Pc bound to PSI did not take into account the effect of the dissociation constants. Equation 14 is similar to an expression given by Dutton and Wilson (1974) for the midpoint potential of a redox couple in the presence of any reagent that has a different binding affinity to the oxidized and the reduced form. It should be pointed out that the value of E_m^{app} in eq 14 is between the values of E_m^{fr} and E_m^{bd} and that the shape of the titration curve follows that of Nernst's equation at least for $[Pc_{tot}] \gg [P700_{tot}]$ (see Appendix) in agreement with the experimental results in Figure 4A.

Redox state sensitive binding has also been reported for the interaction of soluble c-type cytochromes with the cyt bc_1 complex from beef heart mitochondria (Speck & Margoliash, 1984) and with bacterial reaction centers of *Rhodobacter sphaeroides* (Moser & Dutton, 1988). These studies using gel filtration to determine particle sizes (Speck & Margoliash, 1984) and direct measurement of the midpoint potential of cyt *c* in the presence and absence of reaction centers (Moser & Dutton, 1988) indicated multiple binding sites for cyt *c* which may not all be involved in electron transfer. The approach presented here specifically probes reduced Pc functionally bound to PSI.

What Are the Interactions Tuning the Midpoint Redox Potential of the Cofactors in the Complex? Besides the chemical nature of the redox cofactor, it is the protein environment and the free energy of solvation that have a major impact on the midpoint potential *in situ*. This includes the interaction of the redox cofactor in its different oxidation states with charges of the protein, induced dipoles and the surrounding solvent. The question of interest is, how the formation of the complex does affect each of these contributions to the free energy of the redox state transition. In the complex between Pc and PSI the net negative charge of Pc being decreased by one after oxidation should diminish the attraction of Pc by the positive charges of subunit PsaF (Ratajczak et al., 1988; Hippler et al., 1989), in agreement with the dissociation constants $K_D^{I} < K_D^{II}$. Thus, a more positive electrostatic field at the copper center in the complex should indeed favor the reduced over the oxidized state and increase the redox potential as compared to that in solution. This is consistent with the effect of modifications introducing positive charges near the conserved negative patch of Pc which increased the redox potential of soluble Pc by about

30−40 mV (Burkey & Gross, 1982; Sigfridsson et al., 1995; Christensen et al., 1993).

Another effect of the complex formation on the redox potential is related to the short distance of the net positive charge of Cu^{2+} in oxidized Pc to the hydrophobic patch at the protein surface (Guss & Freeman, 1983). This positive charge of the oxidized copper center has been shown to induce a significant electrostatic field in the protein local environment at the hydrophobic surface (Durell et al., 1990; Gross, 1993). It should contribute more to the solvation energy of Pc than the charge of Cu^{+} which is compensated by the negative thiolate ligand of Cys84. Therefore, replacing the high dielectric medium of water in this hydrophobic docking region by a low dielectric medium in the complex will destabilize the oxidized form and contribute to the increase in the redox potential of Pc when it is bound to PSI. The extent of solvent exposure has been identified as one of the major factors modulating the redox midpoint potential in the tetraheme cyt subunit of the bacterial reaction center from *Rhodopseudomonas viridis* (Gunner & Honig, 1991) and in soluble c-type cytochromes (Churg & Warshel, 1986; Dolla et al., 1994).

Redox Potential of P700 in the Complex. Similar to the redox state of Pc the oxidation of P700 may also affect the binding affinity of Pc. The dissociation constant of oxidized Pc when P700 is oxidized, $K_D^{II,+} = 102\ \mu M$, is higher by a factor of 2.6 as compared to the value of K_D^{II} when P700 is reduced. This indicates an increase of the redox potential of P700 by about 25 mV when Pc^{II} is bound to PSI (*cf.* eq 13). The increase should have been observed in the redox titration in Figure 4B because Pc was almost completely oxidized during the titration of the total amplitude of P700. However, the midpoint potential of 475 mV for P700/$P700^{+}$ is close to that found with PSI without bound Pc (not shown) and is consistent with previous reports (Sétif & Mathis, 1980; Rutherford & Heathcote, 1985; *cf.* Golbeck, 1987). In this experiment the total amplitude results from 40% of total PSI without and 60% with cross-linked Pc. The latter fraction may have contributed only a negligible increase at the potentials reached with hexacyanoferrate(III).

We tentatively attribute this effect of the P700 oxidation state on the binding of Pc^{II} to a potential of 25 mV of $P700^{+}$ in the electrostatic field of bound Pc^{II}. Assuming the positive charge of $P700^{+}$ and of the oxidized Cu center at a center to center distance of 20 (Fromme et al., 1994) and 23 Å (M. Hippler, F. Drepper, and W. Haehnel, unpublished result; Hippler, 1994), an average relative dielectric constant ϵ of 29 and 25, respectively, can be estimated from Coulomb's law. A value for ϵ of 19 has been estimated between cyt c_{559} in the tightly bound tetraheme subunit and the primary donor of *R. viridis* reaction centers spaced at 21 Å (Gao et al., 1990). The agreement suggests that the electrostatic interaction between Cu^{II} and $P700^{+}$ can account for the observed binding properties of Pc^{II}. It seems likely that additional contributions from other fixed charges of Pc as those of the negative patch or removal of solvent molecules have a minor influence on the $P700^{+}$/P700 midpoint potential. Therefore, although we have not measured directly the effect of P700 oxidation on the binding constants of Pc^{I}, this seems to be additional support for our assumption of a negligible difference between the dissociation constants K_D^{I} and $K_D^{I,+}$.

Driving Force and Equilibrium of Electron Transfer. How can the measured midpoint redox potentials be related to the free energy of the reaction, $\Delta G°$, for the electron transfer within the complex? Changes in the electrostatic interaction between the reactants have to be considered (Case & Parson, 1971). It is useful to discuss the electron transfer $Pc^{I}\cdot P700^{+} \rightarrow Pc^{II}\cdot P700$ as a sequence of two processes: (i) reduction of $P700^{+}$ in the presence of Pc^{I}, $Pc^{I}\cdot P700^{+} \rightarrow Pc^{I}\cdot P700$, and (ii) oxidation of Pc^{I} in the presence of P700, $Pc^{I}\cdot P700 \rightarrow Pc^{II}\cdot P700$. The first part does not correspond to a free energy change that could be measured in an equilibrium redox titration. However, assuming the binding of Pc^{I} to have only a negligible effect on the E_m of $P700^{+}$/P700 (see above), the E_m measured without bound Pc of about 475 mV (*cf.* Figure 4B and discussion above) can be used instead to describe the energetics of this process. The second part of the reaction corresponds approximately to the redox titration of Pc^{I}/Pc^{II} within the complex and can be characterized by an E_m between 420 and 405 mV as measured for the cross-linked (Figure 4B) and the non-covalent complex (Figure 4A and discussion above), respectively. The difference between these values, ΔE_m, of 55−70 mV is considerably smaller than that between soluble Pc and P700 of about 120 mV. Converting ΔE_m to the free energy of the electron transfer reaction $\Delta G°$ defines the driving force, $\Delta G° = -F\Delta E_m$ (F, Faraday constant), for the intracomplex electron transfer in the range between −5.3 and −6.7 kJ mol^{-1}. The value of the equilibrium constant K_{eq} of the intracomplex electron transfer, $K_{eq} = \exp(-\Delta G°/RT)$, is estimated to be about 10. It is of note that this conversion implies the electrostatic interaction between the cofactors $P700^{+}$ and Pc^{I} to be of equal magnitude as that between P700 and Pc^{II}.

As a consequence of this low K_{eq} value the rapid intracomplex electron transfer with the 11 μs half-life would be limited to about 89% of total $Pc^{I}\cdot P700^{+}$ formed by the flash. This fraction is similar to that of the maximal relative amplitude of the fast component $A(1)$ ranging between 0.83 and 0.92 (Figure 2A) as indicated by the factor of proportionality f between $A(1)$ and the concentration of the complex [$Pc^{I}\cdot P700$] in the dark (eq 6). Thus, the good agreement suggests that the major limitation of the fast turnover is set by the redox potentials and that total PSI does form a functional complex with Pc^{I}. As compared to the midpoint potentials in solution, the driving force of the electron transfer is diminished but with the advantage of a preferential binding of reduced rather than oxidized Pc in favor of an efficient electron transfer through PSI.

Process of Docking as an Additional Kinetic Step? Different from a reaction of small ions in solution, several interactions between proteins may account for deviations from an ideal model. (i) The process of docking can involve a local diffusional step in a binding niche. For Pc we estimate a negligible time of 0.1 μs for a diffusional jump across its own diameter in water. (ii) Substrate inhibition may account for a decrease of the second-order rate constant [*cf., e.g.,* Margoliash and Bosshard (1983)]. This should be indicated in Figure 2B by a decreasing slope at increasing concentrations of Pc, but is not observed. (iii) There may be an additional but nonproductive binding or recognition site from which Pc moves to the productive one. This is similar to the proposal by Marcus and Sutin (1985) that reorientation of a protein that is necessary to form a properly oriented pair from the primary encounter complex could introduce a rate limitation. An additional kinetic step during the docking of Pc to PSI has been suggested by Bottin and Mathis (1985) analogous to the reaction of soluble cyt c_2

with reaction centers of purple bacteria [*e.g.*, Overfield et al. (1979, 1980a,b), Moser and Dutton (1988), and Tiede et al. (1993)]. This conclusion was based on an observation that in PSI particles isolated with digitonin not more than 30% of total P700 showed a fast kinetic component at high concentrations of Pc while the remainder was reduced with a limiting half-life of 110 μs. It is in contradiction to the data in this paper and those found with intact chloroplasts (Haehnel et al., 1989). A rate-limiting step during the docking of Pc in this "three-state" model has also been used recently by Sigfridsson et al. (1995) to model the $P700^+$ reduction kinetics measured at 830 nm. However, none of these studies has included the electron transfer equilibrium in the kinetic analysis. From our data we conclude that the limiting half-life of the slow kinetic component can be explained by the simplest kinetic ("two-state") model if the actual equilibrium of the electron transfer reaction and the release of the product, *i.e.*, oxidized Pc, is taken into account. Thus, we do not observe a kinetic contribution of the docking process. Although not all alternative possibilities can be excluded our results from several independent experiments are consistent with the mechanism in Scheme 1.

Release of Oxidized Plastocyanin Limits the Turnover of P700. An ideal second-order reaction between Pc^I and $P700^+$ should show for increasing concentrations of Pc^I a limiting half-life of 11 μs due to the intracomplex electron transfer in contrast to that of 50−60 μs found by extrapolation for about 10% of total $P700^+$ (Figure 2A,B). However, even at extreme concentrations of Pc^I when total PSI is converted to $Pc^I{\cdot}P700^+$ by a flash, the small equilibrium constant K_{eq} limits the electron transfer in the complex, leaving some $Pc^I{\cdot}P700^+$ in equilibrium with $Pc^{II}{\cdot}P700$. Although the dissociation of $Pc^I{\cdot}P700^+$ with $k_{off}^{I,+}$ may diminish the amplitude of the fast component, it has no effect at "infinite" concentrations of Pc^I. The reduction of $P700^+$ can only proceed if $Pc^{II}{\cdot}P700$ is removed from the equilibrium by dissociation of Pc^{II} (Scheme 1b). Therefore the limiting half-life of ca. 60 μs should indicate the value of the rate constant k_{off}^{II} (*i.e.*, ca. 12×10^3 s^{-1}) which is in good agreement with the value of 9.2×10^3 s^{-1} fitted to the amplitude of the fast component after the second of two flashes (Figure 6).

Our data indicate that the release of oxidized Pc from the binding site is prerequisite for a subsequent turnover of PSI. Since the electron transfer from soluble Pc^I to the cross-linked complex is more than 3 orders of magnitude slower than that to PSI with a free Pc binding site, a functional involvement of a second binding site is rather unlikely. In addition, cross-linking to a second site of PSI has not been found (Hippler et al., 1990). Thus, the release of oxidized Pc preceding the binding of a free reduced Pc limits the turnover of PSI at high concentrations of Pc^I. This dissociation seems also to limit the electron transfer from the cyt *bf* complex to PSI in intact thylakoids (Drepper, 1994). It is evident that the release of oxidized Pc, even being about 2.5 times faster than that of reduced Pc ($k_{off}^{II,+} > k_{off}^{I,+}$), is important for a fast electron transport. At the same time the binding of reduced Pc is faster by about the same factor than that of oxidized Pc ($k_{on}^{II} < k_{on}^{I}$), both being advantageous for a fast turnover of PSI. The accelerated release of Pc^{II} helps also to diminish the back electron transfer from P700 to Pc^{II} in the complex.

Implications for Electron Transport in Thylakoids. In intact spinach chloroplasts and in the green alga *Chlorella sorokiniana* the reduction of 95% of total P700 after a laser flash by monophasic kinetics, with a half-life of 11 and 4 μs (Haehnel et al., 1989; Delosme, 1991), respectively, indicates that also *in vivo* total PSI can exist as an uniform productive complex with Pc. Table 1 summarizes the values estimated from our experiments. We present a nearly complete set of data for two preparations of PSI, one with Chl *a*/Chl *b* ≈ 10 of a purified PSI complex with an intact binding site of Pc and another with Chl *a*/Chl *b* ≈ 4 of PSI associated with a larger fraction of light-harvesting proteins. Although the rate constants of the release of Pc (k_{off}^{I}, k_{off}^{II}, $k_{off}^{II,+}$) agree within the accuracy of our experiments, the major difference between the two preparations can be identified as a difference between the binding constants (k_{on}^{I}, k_{on}^{II}) by a factor of about 3−4. This explains also the difference between the dissociation constants ($K_D = k_{off}/k_{on}$).

The complex with a high value of Chl *a*/Chl *b* and the lowest value of 6−8 μM reported so far for K_D^I with spinach PSI is well defined for studies of the electron transfer. However, the preparation with the lower Chl *a*/Chl *b* ratio may provide conditions closer to those in intact membranes. The difference in the second-order binding process may be due to a repulsion of Pc during the binding process by surface charges near PSI. It is important to note that at the membrane (i) the limiting release of Pc^{II} is not affected and (ii) the value of $K_D^{II,+}$ is close to that of the concentration of Pc in thylakoids (Whitmarsh, 1986). Therefore, under oxidizing conditions a considerable fraction of PSI would not carry a bound Pc in contrast to reducing conditions. The additional free Pc^{II} would be available for reduction at the cyt *bf* complex. The environment of PSI in the membrane could modulate the binding properties of Pc in favor of the electron transport through the cyt *bf* complex. For a more quantitative discussion the dissociation constants in intact membranes and at low lumenal pH values have to be known. The rate constants at the cyt *bf* complex are more difficult to measure than those at PSI, but the knowledge of the rate-limiting release of oxidized Pc from PSI may help to understand more details of the electron transfer kinetics. In addition, the optimized binding and release of reduced and oxidized Pc, respectively, at the expense of the driving force in the bound state may be related to the reorganization energy of the electron transfer and is under investigation.

ACKNOWLEDGMENT

Discussions of theoretical aspects with Bill Parson and help with the figures by Jan Reichert are gratefully acknowledged.

APPENDIX

The amplitude of the 11 μs component of the $P700^+$ reduction kinetics indicates approximately the concentration of the complex between reduced Pc and PSI, $[Pc^I{\cdot}P700]$. This concentration as a function of the ambient redox potential is not directly related by Nernst's equation to the midpoint potential of the couple $[Pc^I{\cdot}P700]/[Pc^{II}{\cdot}P700]$. We have to consider the dissociation constants K_D^I and K_D^{II} of the equilibrium between reduced and oxidized Pc and PSI given by eqs 4 and 8, respectively, as well as Nernst's equation

for bound Pc (*cf.* eq 12b)

$$\frac{[Pc^{II}\cdot P700]}{[Pc^{I}\cdot P700]} = 10^{(E - E_m{}^{bd})/59mV} = B \qquad (A1)$$

where B is introduced as a shorthand symbol for the ratio of oxidized over reduced bound Pc. Total concentrations of Pc and P700 are given by

$$[Pc_{tot}] \approx [Pc^{II}] + [Pc^{I}] \qquad (A2)$$

$$[P700_{tot}] = [P700] + [Pc^{II}\cdot P700] + [Pc^{I}\cdot P700] \qquad (A3)$$

Note that the only approximation used throughout this derivation is introduced by eq A2 which is true for $[Pc_{tot}] \gg [P700_{tot}]$.

The amount of oxidized Pc in the bound state cannot be observed in the experiments. Therefore the ratio B is not known. We write the apparent ratio

$$\frac{[Pc^{I}\cdot P700]_{max} - [Pc^{I}\cdot P700]}{[Pc^{I}\cdot P700]} = \frac{[Pc^{I}\cdot P700]_{max}}{[Pc^{I}\cdot P700]} - 1 \equiv A \qquad (A4)$$

The maximum concentration of the complex between reduced Pc and PSI is found when Pc is totally reduced ($[Pc^{I}] = [Pc_{tot}]$) and follows from eq 4 as given by eq A5

$$[Pc^{I}\cdot P700]_{max} = \frac{[P700_{tot}]([Pc_{tot}]/K_D{}^{I})}{1 + ([Pc_{tot}]/K_D{}^{I})} \qquad (A5)$$

whereas the concentration of $[Pc^{I}\cdot P700]$ as a function of the redox potential can be obtained by solving the system of eqs 4, 8, A1−A3. By substituting eqs A2 and A3 into eqs 4, 8, and A1, these can be rewritten as

$$K_D{}^{I}[Pc^{I}\cdot P700] = [Pc_{tot}][P700] - [Pc^{II}][P700] \qquad (A6)$$

$$K_D{}^{II}[P700_{tot}] - K_D{}^{II}[Pc^{I}\cdot P700] - K_D{}^{II}[P700] = [Pc^{II}][P700] \qquad (A7)$$

$$(B + 1)[Pc^{I}\cdot P700] = [P700_{tot}] - [P700] \qquad (A8)$$

Taking the sum of eqs A6, A7, and A8 multiplied by ($[Pc_{tot}] + [P700_{tot}]$), this converts to

$$[Pc^{I}\cdot P700] = \frac{[Pc_{tot}][P700_{tot}]}{K_D{}^{I} - K_D{}^{II} + ([Pc_{tot}] + K_D{}^{II})(B + 1)} \qquad (A9)$$

Substituting eqs A5 and A9 into eq A4 and rearranging gives

$$A = B\frac{K_D{}^{II} + [Pc_{tot}]}{K_D{}^{I} + [Pc_{tot}]} \qquad (A10)$$

Finally, combining eq A10 with A1 we arrive at a Nernst-type equation

$$A = 10^{(E - E_m{}^{app})/59mV} \qquad (A11)$$

with an apparent midpoint potential

$$E_m{}^{app} = E_m{}^{bd} - 59mV\ \log\left(\frac{K_D{}^{II} + [Pc_{tot}]}{K_D{}^{I} + [Pc_{tot}]}\right) \qquad (A12)$$

Thus, the amount of bound reduced Pc as a function of the ambient redox potential follows a Nernst-type equation exhibiting an apparent midpoint potential given by eq A12. When $K_D{}^{II} >$ (or $<$) $K_D{}^{I}$, the apparent midpoint potential would be smaller (greater) than the actual redox potential of the couple $[Pc^{I}\cdot P700]/[Pc^{II}\cdot P700]$. The value of $E_m{}^{app}$ depends on the concentration of Pc unless the binding site is saturated, *i.e.*, $[Pc_{tot}] \gg K_D{}^{I}$ and $\gg K_D{}^{II}$, when it approaches $E_m{}^{bd}$.

REFERENCES

Allen, J. P., Feher, G., Yeates, T. O., Komiya, H., & Rees, D. C. (1987) *Proc. Natl. Acad. Sci. U.S.A. 84*, 5730−5734.

Armstrong, F. A., Hill, H. A. O., Oliver, B. N., & Whitford, D. (1985) *J. Am. Chem. Soc. 107*, 1473−1476.

Bengis, C., & Nelson, N. (1977) *J. Biol. Chem. 252*, 4564−4569.

Bottin, H., & Mathis, P. (1985) *Biochemistry 24*, 6453−6460.

Bottin, H., & Mathis, P. (1987) *Biochim. Biophys. Acta 892*, 91−98.

Boxer, S. G. (1990) *Annu. Rev. Biophys. Chem. 19*, 267−299.

Burkey, K. O., & Gross, E. L. (1982) *Biochemistry 21*, 5886−5890.

Case, G. D., & Parson, W. W. (1971) *Biochim. Biophys. Acta 253*, 187−202.

Christensen, H. E. M., Conrad, L. S., & Ulstrup, J. (1993) *Arch. Biochem. Biophys. 301*, 385−390.

Churg, A. K., & Warshel, A. (1986) *Biochemistry 25*, 1675−1681.

Clark, W. M. (1960) *Oxidation−Reduction Potentials of Organic Systems*, Williams and Wilkins, Baltimore, MD.

Collyer, C. A., Guss, J. M., Sugimura, Y., Yoshizaki, F., & Freeman, H. C. (1990) *J. Mol. Biol. 211*, 617−632.

Deisenhofer, J., Epp, O., Miki, K., Huber, R., & Michel, H. (1985) *Nature 318*, 618−624.

Delosme, R. (1991) *Photosynth. Res. 29*, 45−54.

Dolla, A., Blanchard, L., Guerlesquin, F., & Bruschi, M. (1994) *Biochimie 76*, 471−479.

Drepper, F. (1994) Ph.D. Dissertation, Albert-Ludwigs-Universität Freiburg, Germany.

Durell, S. R., Labanowski, J. K., & Gross, E. L. (1990) *Arch. Biochem. Biophys. 277*, 241−254.

Dutton, P. L., & Wilson, D. F. (1974) *Biochim. Biophys. Acta 346*, 165−212.

Fromme, P., Schubert, W.-D., & Krauss, N. (1994) *Biochim. Biophys. Acta 1187*, 99−105.

Gao, J.-L., Shopes, R. J., & Wraight, C. A. (1990) *Biochim. Biophys. Acta 1015*, 96−108.

Golbeck, J. H.(1987) *Biochim. Biophys. Acta 895*, 167−204.

Gross, E. L. (1993) *Photosynth. Res. 37*, 103−116.

Gunner, M. R., & Dutton, P. L. (1989) *J. Am. Chem. Soc. 111*, 3400−3412.

Gunner, M. R., & Honig, B. (1991) *Proc. Natl. Acad. Sci. U.S.A. 88*, 9151−9155.

Guss, J. M., & Freeman, H. C. (1983) *J. Mol. Biol. 169*, 521−563.

Guss, J. M., Harrowell, P. R., Murata, M., Norris, V. A., & Freeman, H. C. (1986) *J. Mol. Biol. 192*, 361−387.

Haehnel, W. (1986) in Photosynthesis III: Photosynthetic Membranes and Light Harvesting Systems, *Encyclopedia of Plant Physiology, New Series* (Staehelin, L. A., & Arntzen, C. J., Eds.) Vol. 19, pp 547−559, Springer-Verlag, Berlin.

Haehnel, W., Döring, G., & Witt, H. T. (1971) *Z. Naturforsch. 26B*, 1171−1174.

Haehnel, W., Pröpper, A., & Krause, H. (1980) *Biochim. Biophys. Acta 593*, 384−399.

Haehnel, W., Ratajczak, R., & Robenek, H. (1989) *J. Cell Biol. 108*, 1397−1405.

Haehnel, W., Jansen, T., Gause, K., Klösgen, R. B., Stahl, B., Michl, D., Huvermann, B., Karas, M., & Herrmann, R. G. (1994) *EMBO J. 13*, 1028−1038.

He, S., Modi, S., Bendall, D. S., & Gray, J. C. (1991) *EMBO J. 10*, 4011−4016.

Hippler, M. (1994) Ph.D. Dissertation, Albert-Ludwigs-Universität Freiburg, Germany.
Hippler, M., Ratajczak, R., & Haehnel, W. (1989) *FEBS Lett. 250*, 280−284.
Hippler, M., Ratajczak, R., & Haehnel, W. (1990) in *Current Research in Photosynthesis*, Proceedings of the 8th International Congress on Photosynthesis, Stockholm, Sweden, August 6−11, 1989 (Baltscheffsky, M., Ed.) Vol. 2, pp 675−678, Kluwer Academic Publishers, Dordrecht, The Netherlands.
Hiyama, T., & Ke, B. (1972) *Biochim. Biophys. Acta 267*, 160−171.
Katoh, S., Shiratori, I., & Takamiya, A. (1962) *J. Biochem. 51*, 32−40.
Lin, X., Williams, J. C., Allen, J. P., & Mathis, P. (1994) *Biochemistry 33*, 13517−13523.
Marcus, R. A., & Sutin, N. (1985) *Biochim. Biophys. Acta 811*, 265−322.
Margoliash, E., & Bosshard, H. R. (1983) *Trends Biochem. Sci. 8*, 316−320.
Moore, J. M., Case, D. A., Chazin, W. J., Gippert, G. P., Havel, T. F., Powls, R., & Wright, P. E. (1988) *Science 240*, 314−317.
Moore, J. M., Lepre, C. A., Gippert, G. P., Chazin, W. J., Case, D. A., & Wright, P. E. (1991) *J. Mol. Biol. 221*, 533−555.
Moser, C. C., & Dutton, P. L. (1988) *Biochemistry 27*, 2450−2461.
Moser, C. C, Keske, J. M., Warncke, K., Farid, R. S., & Dutton, P. L. (1992) *Nature 355*, 796−802.
Nordling, M., Sigfridsson, K., Young, S., Lundberg, L. G., & Hansson, Ö. (1991) *FEBS Lett. 291*, 327−330.
Olsen, L. F., & Cox, R. P. (1982) *Biochim. Biophys. Acta 679*, 436−443.
Overfield, R. E., Wraight, C. A., & DeVault, D. (1979) *FEBS Lett. 105*, 137−142.
Overfield, R. E., & Wraight, C. A. (1980a) *Biochemistry 19*, 3322−3327.
Overfield, R. E., & Wraight, C. A. (1980b) *Biochemistry 19*, 3328−3334.
Porra, R. J., Thompson, W. A., & Kriedemann, P. E. (1989) *Biochim. Biophys. Acta 975*, 384−394.
Ratajczak, R., Mitchell, R., & Haehnel, W. (1988) *Biochim. Biophys. Acta 933*, 306−318.
Redinbo, M. R., Cascio, D., Choukair, M. K., Rice, D., Merchant, S., & Yeates, T. O. (1993) *Biochemistry 32*, 10560−10567.
Rutherford, A. W., & Heathcote, P. (1985) *Photosynth. Res. 6*, 295−316.
Sanderson, D. G., Anderson, L. B., & Gross, E. L. (1986) *Biochim. Biophys. Acta 852*, 269−278.
Sétif, P., & Mathis, P. (1980) *Arch. Biochem. Biophys. 204*, 477−485.
Sigfridsson, K., Hansson, Ö., Karlsson, B. G., Baltzer, L., Nordling, M., & Lundberg, L. G. (1995) *Biochim. Biophys. Acta 1228*, 28−36.
Speck, S. H., & Margoliash, E. (1984) *J. Biol. Chem. 259*, 1064−1072.
Sykes, A. G. (1990) *Struct. Bonding 75*, 175−224.
Tiede, D. M., Vashishta, A.-C., & Gunner, M. R. (1993) *Biochemistry 32*, 4515−4531.
Venturoli, G., Mallardi, A., & Mathis, P. (1993) *Biochemistry 32*, 13245−13253.
Whitmarsh, J. (1986) in Photosynthesis III; Photosynthetic Membranes and Light Harvesting Systems, *Encyclopedia of Plant Physiology, New Series* (Staehelin, L. A., & Arntzen, C. J., Eds.) Vol. 19, pp 508−527, Springer-Verlag, Berlin.
Wynn, R. M., & Malkin, R. (1988) *Biochemistry 27*, 5863−5869.

BI951471E